

## Tire Modeling with Nonlinear Behavior for Vehicle Dynamic Studies

S. Sadeghi<sup>1</sup> and M.T. Ahmadian\*

In this paper, a nonlinear tire model based on the elliptic concept and tire Calspan data has been developed. The effect of cornering force and aligning moment as a function of slip and camber (inclination) angles, normal load, tire adhesion characteristics and skid number are studied. Furthermore, in this model, the rolling resistant effect has been considered. Through this simple tire model, the tire behavior as well as the experimental results are represented.

### INTRODUCTION

One of the main sources of nonlinearities in vehicle dynamics is the tire, whose behavior can be extraordinarily complex. It is clear that the vehicle motion depends on tire forces and at the same time tire forces depend on vehicle motion. These forces and moments are fundamentally important to stability, control and guidance of vehicles. Hence, the handling characteristics of a given vehicle cannot be predicted unless the forces and moments acting on the tire road contact area are well described and integrated into the vehicle model.

During the last two decades, numerous studies on tire characteristics and modeling techniques have been performed. Some studies on tire modeling have been based on the elastic deformation and compliance of carcass [1,2]. Other studies have been based on experimental results and pure analytical modeling, by either fitting curves to measurement points [3-5] or assuming suitable pressure distribution in the contact area [6].

### COORDINATE SYSTEM

One of the commonly used axis systems recommended by SAE is shown in Figure 1 [7]. The origin of the axis system is the center of tire contact. The X-axis is the intersection of the wheel plane and the ground plane with the positive direction forward. The Z-axis

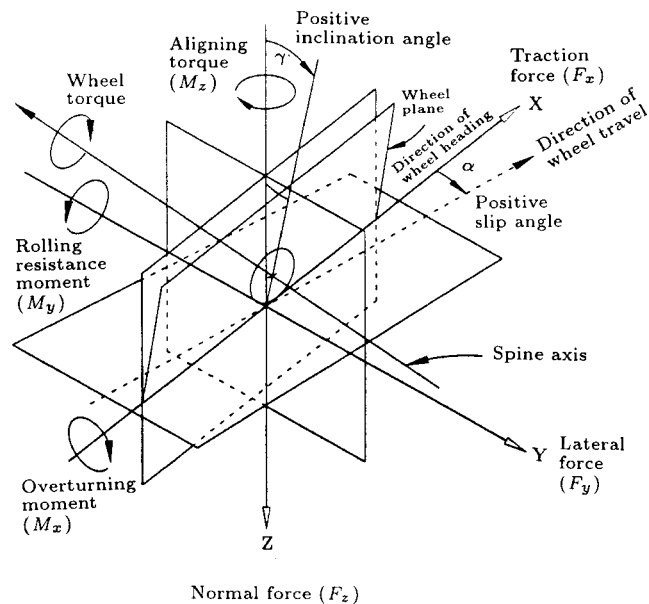


Figure 1. SAE tire coordinate system.

is perpendicular to the ground plane with a positive direction downward. The Y-axis is in the ground plane with a direction that makes the right hand orthogonal coordinate system. A tire is subjected to forces and moments acting on it by the road surface as shown in Figure 1. Longitudinal force,  $F_x$ , is caused by traction, braking or rolling resistance. Since tire heading and tire traveling directions do not coincide, lateral force,  $F_y$ , is produced through lateral slip due to the slip angle  $\alpha$ . Lateral force is also caused by camber angle  $\gamma$ . The sum of these two effects defines the cornering force. Aligning moment,  $M_z$ , is about Z-axis as the product of shear force (sum of the lateral and longitudinal forces) and

1. Department of Mechanical Engineering, Sharif University of Technology, Tehran, I.R. Iran.

\*. Corresponding Author, Department of Mechanical Engineering, Sharif University of Technology, Tehran, I.R. Iran.

its moment arm with respect to the tire axis in XY-plane. The overturning moment,  $M_x$ , is defined about X-axis and since it is very small, it is ignored in most studies. The rolling resistance moment,  $M_y$ , about Y-axis is caused by traction and braking torque and is zero in free rolling.

## MODELING

The maximum lateral force (longitudinal force) which a tire can generate, with no braking or traction force (lateral force) applied, is given by:

$$\begin{aligned} F_{x_{\max}} &= \mu_x F_z, \\ F_{y_{\max}} &= \mu_y F_z, \end{aligned} \quad (1)$$

where  $\mu_x$  and  $\mu_y$  are the peak friction coefficients between the tire tread and road surface. These complex characteristics depend on the normal load, velocity, tread rubber material, road condition and temperature that can be expressed by tire Calspan data and normal load :

$$\begin{aligned} \mu_x &= (p_0 + p_1 F_z + p_2 F_z^2) \frac{SN_0}{SN_T}, \\ \mu_y &= (b_3 + b_1 F_z + b_4 F_z^2) \frac{SN_0}{SN_T}, \end{aligned} \quad (2)$$

where  $p_i (i = 0 - 2)$  and  $b_i (i = 1, 3, 4)$  are Calspan data, expressing peak lateral and longitudinal friction coefficients.  $SN_T$  is the skid number of Calspan test and  $SN_0$  is the tire skid number on road which can be written as:

$$SN_0 = 100\mu_{nom}, \quad (3)$$

where  $\mu_{nom}$  is the nominal road friction coefficient.

It is clear that an object moves and slides in the direction of resultant applied forces and friction force behavior is based on a circular, (if friction coefficients are equal in all directions  $F_x^2 + F_y^2 = F_{\max}^2$ ) or elliptical concept. Therefore, the maximum permissible lateral force is reduced by the effect of braking or traction (longitudinal) force. This effect, considering Equation 1, can be calculated as:

$$\frac{F_x^2}{F_{x_{\max}}^2} + \frac{F_y^2}{F_{y_{\max}}^2} = 1 \Rightarrow Y = \sqrt{F_{y_{\max}}^2 - \frac{\mu_x^2}{\mu_y^2} F_x^2}. \quad (4)$$

Conventionally, the cornering stiffness which strongly depends on the normal load is defined by the following empirical relation:

$$C_\alpha = \frac{\partial F_y}{\partial \alpha} \Big|_{\alpha=0} = a_0 + a_1 F_z - \left( \frac{a_1}{a_2} \right) F_z^2, \quad (5)$$

where  $F_z$  represents normal tire load and  $a_i (i = 0 - 2)$  are Calspan tire data which express variation of lateral force versus slip angle.

The relation between lateral force and slip angle is fundamentally important to the directional control and stability of the road vehicle. Lateral force increases by increasing slip angle and saturates at large slip angles. The shape of this curve is the same for all tires and only its scale can be changed. By curve fitting the experimental data, the following saturation function is obtained:

$$f(\bar{\alpha}) = \begin{cases} 1 & \bar{\alpha} \geq 3 \\ \bar{\alpha} - \frac{1}{3}|\bar{\alpha}| + \frac{1}{27}\bar{\alpha}^3 & |\bar{\alpha}| < 3 \\ -1 & \bar{\alpha} \leq -3 \end{cases} \quad (6)$$

where  $\bar{\alpha}$  is the corrected slip angle:

$$\bar{\alpha} = \frac{\alpha}{Y} C_\alpha. \quad (7)$$

The cornering force generated by the tire is a function of normal load  $F_z$ , slip angle  $\alpha$ , maximum allowable lateral force  $Y$ , cornering stiffness  $C_\alpha$ , camber angle  $\gamma$  and camber stiffness  $C_\gamma$  calculated as follow:

$$F_y = f(\bar{\alpha})Y + C_\gamma \gamma, \quad (8)$$

where the first and second terms are the result of side slip and inclination, respectively. In fact, the effect of slip and camber angles are superimposed in this equation. Camber stiffness can be obtained in the same manner:

$$C_\gamma = \frac{\partial F_y}{\partial \gamma} \Big|_{\gamma=0} = a_3 F_z - \left( \frac{a_3}{a_4} \right) F_z^2, \quad (9)$$

where  $a_i (i = 3, 4)$  are Calspan tire data, demonstrating the variation of lateral force versus camber angle.

Since the lateral and longitudinal forces have offset from the origin of coordinate, these forces produce moment about Z-axis which defines 'aligning moment'. By increasing slip angle, the aligning moment increases and then smoothly approaches zero at slip angle  $\alpha^*$ , where lateral force is saturated. Moreover, Gim [2] showed that peak aligning moment takes place at 1/4 of this slip angle. With the above discussion, the following bilinear equations are considered as the basis for the aligning moment:

$$M_z = \begin{cases} n_a \alpha & \alpha < \frac{\alpha^*}{4} \\ \frac{4}{3} \bar{M} \left( 1 - \frac{\alpha}{\alpha^*} \right) & \frac{\alpha^*}{4} < \alpha < \alpha^* \\ 0 & \alpha > \alpha^* \end{cases} \quad (10)$$

$$\begin{cases} \bar{M} = n_a \frac{\alpha^*}{4} \text{ max. aligning moment} \\ \alpha^* = \alpha \Big|_{\bar{\alpha}=3} = \frac{3C_\alpha}{Y} \end{cases}$$

In free rolling, applied wheel torque is zero, but the carcass deflects in the area of the ground contact. As a result of tire distortion, the center of normal pressure is shifted in the direction of rolling and produces a moment about the Y-axis. For equilibrium, there must be a longitudinal force in the contact area which, generally, is known as rolling resistance and can be expressed as:

$$F_{x_{max}} = f_r F_z. \tag{11}$$

$f_r$  is the ratio of rolling resistance to the normal load which defines rolling resistance coefficient. Rolling resistance coefficient is a function of velocity, inflation pressure, tire geometry, type of tire, normal load and shoulder temperature. Based on experimental results [8] for under-rated tire load and inflation pressure on a smooth road, this factor can be evaluated:

for radial type:

$$f_r = 0.0136 + 0.4 \times 10^{-7} V^2 \tag{12a}$$

for Bias type:

$$f_r = 0.0169 + 0.19 \times 10^{-6} V^2. \tag{12b}$$

The tire model response for “Bridgestone P185/70 R13 24 Psi”, with characteristics presented in Table 1, is illustrated in Figures 2 to 6. The relation between lateral force and slip angle is shown in Figure 2. For small slip angle, the lateral force is approximately proportional to slip angle. The slope of this diagram (side force coefficient) decreases at high slip angles where lateral force is saturated. The normal load on the tire strongly influences the cornering characteristics, as shown in Figure 3. For a given slip angle, the

**Table 1.** “Bridgestone P185/70 R13 24 Psi” tire characteristics.

| Parameters  | Value      |
|-------------|------------|
| $a_0$       | 1068       |
| $a_1$       | 11.3       |
| $a_2$       | 2442.73    |
| $a_3$       | 0.31       |
| $a_4$       | -1877      |
| $b_1$       | 0.169 e-3  |
| $b_3$       | 1.04       |
| $b_4$       | 1.69 e-8   |
| $p_0$       | 0.9103     |
| $p_1$       | 7.335 e-8  |
| $p_2$       | -2.272 e-9 |
| $n_\alpha$  | -600       |
| $\mu_{nom}$ | 0.85       |
| $SN_0$      | 85         |

lateral force generally increases with increasing normal load in a nonlinear form. The interaction of the longitudinal and lateral forces and the friction ellipse limit on total force is presented in Figure 4. In Figure 5, variation of cornering characteristic versus

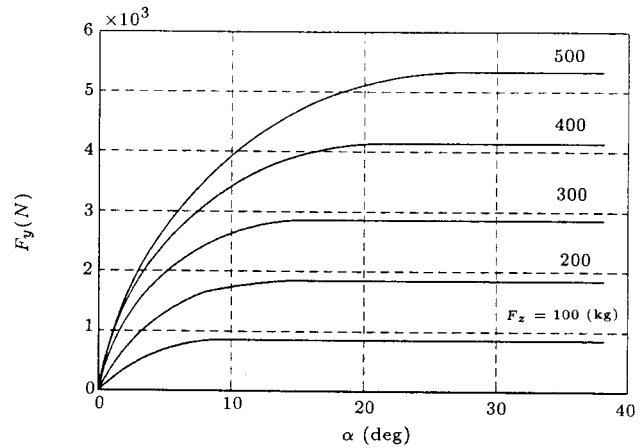


**Figure 2.** Lateral force characteristics vs slip angle.

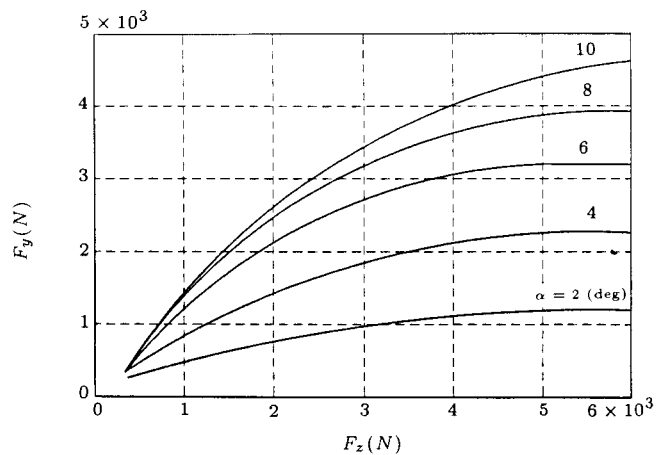


**Figure 3.** Lateral force characteristics vs normal load.

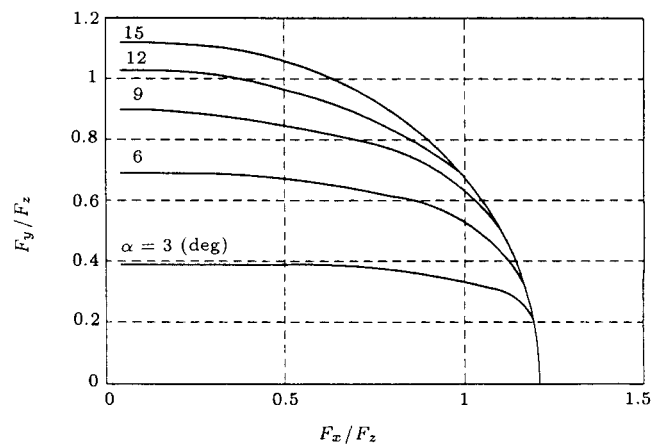


**Figure 4.** Lateral force vs longitudinal force.

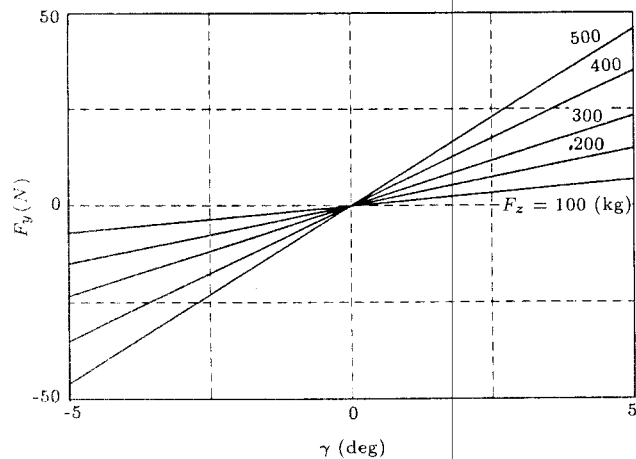


Figure 5. Lateral force characteristics vs camber angle.

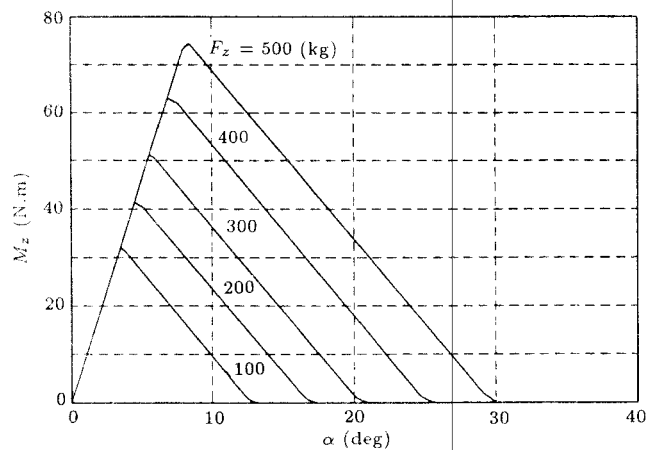


Figure 6. Aligning moment characteristics vs slip angle.

camber angle is shown. The aligning moment versus slip angle is depicted in Figure 6. Aligning moment initially increases and, then, decreases with increasing slip angle.

It is clear that the effect of saturation on side force, normal load, slip and camber angles and traction or braking are very important in handling properties of the vehicle. In maneuvering and braking (traction) and turning and rolling of the body (load transfer due to lateral and longitudinal acceleration), tire behavior is very significant which effects directional stability.

The illustrated tire model response characteristics clearly indicate that the model is capable of predicting the full tire motion operating range. The results obtained using this model compare satisfactorily with the experimental findings [3,8].

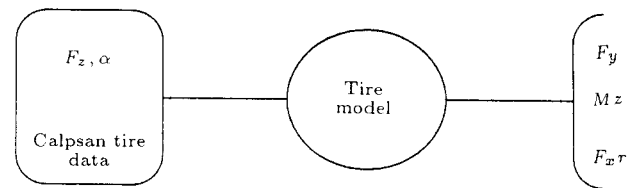


Figure 7. Tire model block diagram.

## CONCLUSION

In this paper, a simple method is described for tire modeling used in vehicle dynamic analysis. This model is based on elliptic friction concept (Equation 4), Calpsan tire data (Equations 2, 5 and 9) and experimental results (Equation 6), which describe dynamic characteristic cornering, aligning moment and rolling resistance effect. The behavior of the tire during combined cornering and braking (traction) is also well predicted. The results indicate that although this model is simple, it provides behavior characteristics comparable to experimental results presented here and in other studies [3,5,8]. Finally, this model can be presented as a block diagram in Figure 7.

## REFERENCES

1. Nikravesh, P.E. and Gwanghun, G. "A three dimensional tire model for steady state simulation of vehicles", S.A.E Paper No. 931913 (1993).
2. Pacejka, H.B. and Sharp, R.S. "Shear force development by pneumatic tires in steady state condition: A review of modeling aspects", *J. of Vehicle System Dynamics*, 20 (1991).
3. Sakai, H. "Theoretical and experimental studies on the dynamic properties of tire", S.A.E Paper No. 870421 (1987).
4. Pacejka, H.B. and Bakker, E. "Tire modeling for use in vehicle dynamic studies", S.A.E Paper No. 870421 (1987).
5. Dieterich, J.S., Wolfgang, P., Marion, G.P. "The BNPS model - An automated implementation of the 'Magic Formula' concept", S.A.E Paper No. 870421 (1987).
6. Allen, R.W. and Szostak, H.T. "Steady state and transient analysis of ground vehicle handling", S.A.E Paper No. 870495 (1987).
7. *SAE Handbook*, Vehicle Dynamic Terminology, 4, SAE J670e (1994).
8. Wong, J.G. *Theory of Ground Vehicles*, John-wiley, New York (1993).